Korean J. Chem. Eng., **23**(5), 847-853 (2006)

Electrochemical properties of Al and Al alloys relevant to corrosion protection in seawater environments

Seong-Jong Kim† and Jae-Yong Ko*

Division of Marine Engineering, *Division of Ocean System Engineering,
Mokpo Maritime University, Mokpo City, Cheonnam 530-729, Korea
(*Received 2 September 2005 • accepted 12 May 2006*)

Abstract−A series of electrochemical experiments on Al alloys were undertaken to determine their optimum protection potentials in seawater. With 1050 and 5456 alloys, passive films form during anodic polarization but are destroyed by the Cl^- in seawater, only to regrow as a result of the self-healing capacity of aluminum. The current density of 5456 Al alloy proved to be lower than that of 1050 as a whole. Any shift to more anodic or cathodic conditions in the potential range of −1.5~−0.68 V resulted in a sudden increase in current density. Current densities in the high-strength 7075 Al alloy showed the greatest values. In contrast, the current densities of 5456 alloy, known to have excellent corrosion resistance in seawater, were the lowest in the range of −0.70~−1.3 V, and we concluded that this potential range offered optimal protection.

Key words: Electrochemical Experiments, Al Alloys, Protection Potentials, Corrosion

INTRODUCTION

Modern trends in production require manufactured goods to be environmentally friendly, easy to recycle, and harmless to the human body, whatever their functional characteristics and economical efficiencies. FRP (fiber-reinforced polymer) ships used with small boats for fishing pose numerous problems from both the environmental and recycling perspectives. In particular, no methods exist to dispose of these ships at the end of their service. The composite FRP materials of which they are constructed is susceptible to fire and is prohibited from use in high-speed passenger ships and cargo boats with gross tonnages in excess of 500 tons, such as those commonly used in coastal navigation. In addition, FRP ships are small. As with wooden vessels, larger craft cannot detect FRP ships by radar since their composite materials reflect radar waves poorly. According to data collected by the Ministry of Maritime Affairs and Fisheries, a large proportion of ship accidents involve these vessels, comprising 72.4% of all marine accidents between 1998 and 2002 and approximately 58% of all collisions involving fishing boats [Cho, 2004]. In light of these considerations, aluminum offers a far better material for ship building than does FRP. It is environmentally friendly, easy to recycle, and provides a high added value to fishing boats. Aluminum craft require less fuel. Developed nations have shown an increasing interest in utilizing Al alloys in ships since environmental restrictions on scrapping FRP ships have become stronger. The use of Al for ships has several advantages. The specific strength of Al ships is higher than that of steel ships. They are capable of high speed, have increased load capacities, greater ease of recycling, and high anticorrosion properties [Kang et al., 2004]. Ships constructed with 5000-series Al alloy suffer little or no corrosion in the marine environment.

†To whom correspondence should be addressed.
E-mail: ksj@mmu.ac.kr

In this paper, we report a number of electrochemical experiments undertaken to determine the optimum conditions for protecting Al alloys in seawater. The results provide reference data relevant to ship design.

EXPERIMENTAL

The main material used in the experiments was 5456 Al alloy, the most commonly used material for ship construction among the 5000-series Al alloys. In addition, 1050 and high-strength Al alloy 7075 were also examined to provide comparative mechanical and electrochemical data. Table 1 gives the mechanical properties and chemical compositions of 1050, 5456-H116 (referred to as 5456 in the following account), and 7075-T6 (referred to as 7075) alloys.

Hardness was measured with a micro-Vickers hardness tester (Mitutoyo, Kawasaki, Japan), with an applied load of 9.807 N, an upkeep time of 10 sec, and a measuring distance of 1 mm. A mean value of 20 measurements was used.

For the electrochemical experiments, the specimens (1050, 5456, and 7075) were mounted in an epoxy resin so as to leave an exposed area of 10 mm^2 that was polished with #600 emery paper. Each specimen was carefully degreased with acetone and distilled water. Corrosion potential was measured over 24 hours at room temperature by using an electrochemical apparatus consisting of a Pt coil as the counter electrode and an Ag/AgCl-saturated KCl reference electrode. A scan rate of 2 mV/sec was applied at room temperature in natural seawater.

Anodic polarization experiments were executed from an open circuit potential (OCP) to a range of −0.5~3.0 V. Cathodic polarization experiments were undertaken from OCP to −2.0 V. The anodic polarization experiments in seawater were carried out in order to investigate the effects on corrosion resistance by an anodic oxide film in the range of 0-5 V. In potentiostatic experiments, a variety of polarization potentials in seawater were applied for 1,200 sec

Table 1. Comparison of the chemical composition and mechanical properties of 1050, 5456-H116, and 7075-T6 Al alloys

(a) Chemical composition (%)

	Si	Fe	Cu	Mn	Mg	Cr	Zn	Ti	Al
1050	0.41	0.36	0.15	0.018	0.029	-	0.06	0.017	98.99
5456-H116	0.08	0.20	0.05	0.79	4.80	0.09	0.09	0.02	Balance
7075-T6	0.09	0.18	1.66	0.03	2.56	0.21	5.57	0.04	Balance

(b) Mechanical properties

	Tensile strength (MPa)	Yield strength (MPa)	Elongation (%)
1050	103.6	108.0	10
5456-H116	534.1	397.9	14
7075-T6	573.3	504.7	11

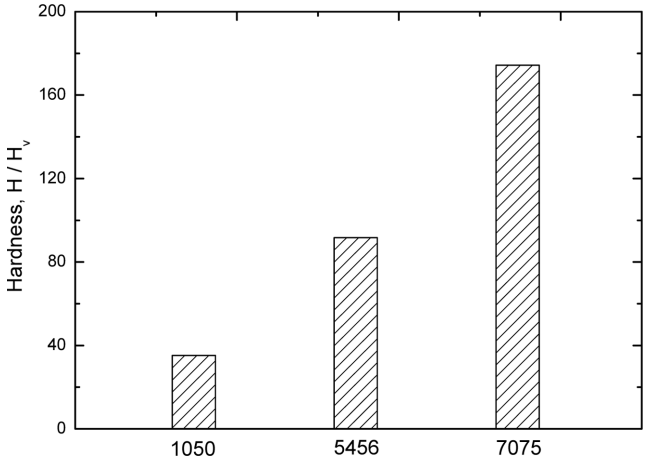

Fig. 1. Comparison of hardness for 1050, 5456 and 7075 Al alloy.

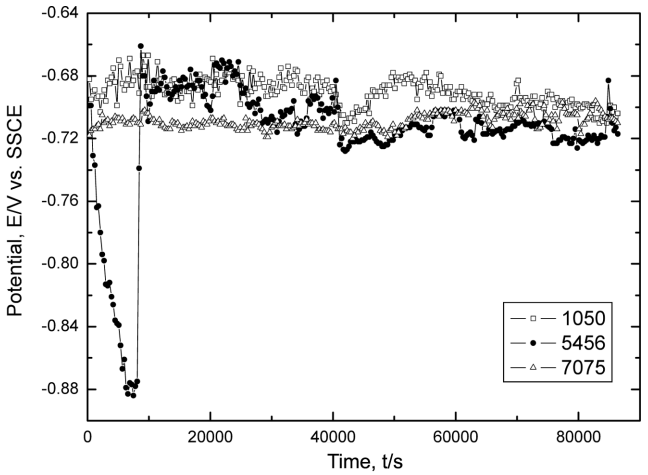

Fig. 2. Variation of potential for 1050, 5456, 7075 specimens during 86400 s in natural sea water solution.

and evaluated in terms of the variations in current density with time and by ascertaining the current density remaining after 1,200 sec at the applied potential. In addition, Tafel analyses were performed under both anodic and cathodic conditions from OCP up to 250 mV in aeration condition. The corrosion potential and corrosion current density were compared with Tafel analytical results obtained from various reference specimens.

RESULTS AND DISCUSSION

Fig. 1 compares the hardness values for the 1050, 5456, and 7075 Al alloys. The hardness of the pure Al (1050) is 35.13, and pure Al displays characteristics of good weldability, with low strength and low hardness. The main additional element in 5456 Al alloy is magnesium. The hardness of this alloy is 91.96. That of 7075 Al is the highest at 174.30, and consequently, this alloy is widely used in the fabrication of aircraft, railroad cars, and other vehicles. However, 7075 Al alloy is prone to stress corrosion cracking and related problems, and has been investigated in order to manage these defects via heat treatment [Inoue et al., 1994; Kanematsu et al., 1986].

The variations in potential in the 1050, 5456, and 7075 specimens during 86,400 sec in seawater are shown in Fig. 2. The corrosion potential of pure Al 1050 retained a steady value following immersion. In contrast, the corrosion potential of 5456 Al alloy abruptly shifted from its value obtained during the earliest stages of immersion because its passive film was destroyed by the action of the Cl^- ion in seawater. The potential after about 8,000 sec was −0.88 mV (vs. Ag/AgCl), but thereafter abruptly increased to −0.69 V, where it remained while another film formed. After about 40,000 sec, a further shift occurred following destruction of the new film by the Cl^-, whereupon the potential again attained a stable value. In contrast, the 7075 Al alloy showed a steady corrosion potential from its earliest stages of immersion.

In summary, pure Al 1050 showed the highest corrosion potential. The potential values for 5456 Al alloy varied with time but were considerably lower than those of the other alloys; the corrosion potential of 7075 Al alloy remained steady from its initial stages of immersion.

Fig. 3 shows the anodic polarization curves for 1050, 5456, and 7075 specimens in seawater. The potentials around open-circuit potential conditions were similar for all specimens. The current densities from OCP to −0.55 V for all three alloys were increased abruptly. Thereafter, the current density in the 7075 Al alloy increased markedly while the current densities of 1050 and 5456 decreased slightly as the potential increased, suggesting that a passive film had developed in the seawater environment. In general, Al and Al alloy do not corrode due to the formation of a film such as Al_2O_3 and $Al_2O_3 \cdot 3H_2O$ in neutral solution. The passive films formed during anodic

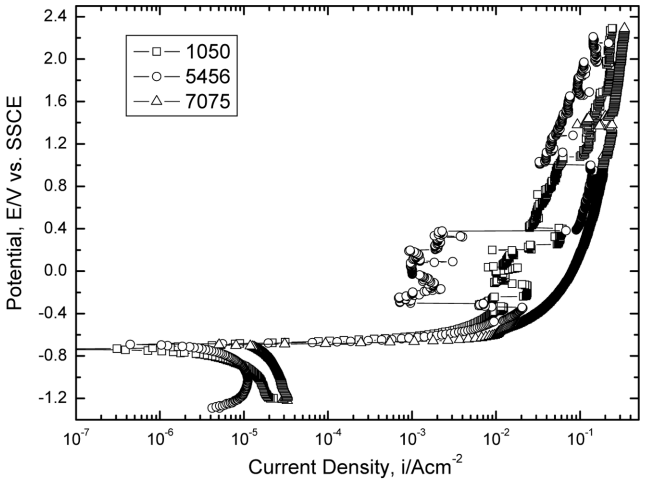

Fig. 3. Comparison of anodic polarization curves for 1050, 5456, 7075 specimens in natural sea water solution.

polarization were subsequently destroyed by the Cl^- in solution. However, the passivity continued to develop due to the self-healing capacity of aluminum. The current density for 5456 Al alloy decreased abruptly in the potential range of −0.3~0.4 V. In contrast, the current density of 7075 Al alloy increased with increasing potential during anodic polarization without passivity developing. On the whole, the current density of 5456 Al alloy remained less than that of 1050. The passivity phenomenon in 7075 Al alloy was not observed by the continuous increase in current density. This alloy was weakened by stress corrosion cracking, and 1050 proved superior to 7075 in this respect. However, 1050 alloy is too weak to be used in ship building, and 5456 Al alloy is most widely used because it is both strong and resistant to stress corrosion cracking in the seawater environment. Until now, stress corrosion cracking characteristics for all specimens are best analyzed by using anodic polarization curves. In the present study, potentiostatic experiments were also undertaken for 1,200 sec and at a variety of applied potentials in order to examine this behavior in detail.

Fig. 4 shows time-current density curves obtained from the potentiostatic analysis of 5456 alloy in seawater. In the following discussion, the shorthand PSa5-A-0.80 means potentiostatic experiment (PSa), 5456 specimen (5), anodic polarization potential (A), and applied potential (−0.80 V). A variation in current density was observed over the entire 1,200 sec of the experiment in the range of −0.80~−0.70 V, but values remained low as shown in Fig. 3. The current densities at −0.80, −0.75, and −0.72 V after 1,200 sec were very low at 5.98×10^{-7}, 7.35×10^{-7}, and 1.74×10^{-7} A/cm^2, respectively. Nonetheless, the current densities over the entire applied potential range of −0.80~−0.72 V were 0.5 times of that found with 1050. The highest value shows after 140 sec at a potential of −0.70 V. After 1,200 sec, the current density was 4.23×10^{-6} A/cm^2.

Fig. 4(b) shows the potentiostatic results in the range of −0.68~−0.50 V. The current density at an applied potential of –0.68 V remained stable from the earliest stages of the experimental run. After 1,200 sec, the current density was 3.4×10^{-4} A/cm^2. In contrast, the current density at −0.65 V increased over the first 50 sec to remain stable thereafter. After 1,200 sec, the value was 2.091×10^{-3} A/cm^2. The current densities for potentials of −0.60 and −0.50 V behaved

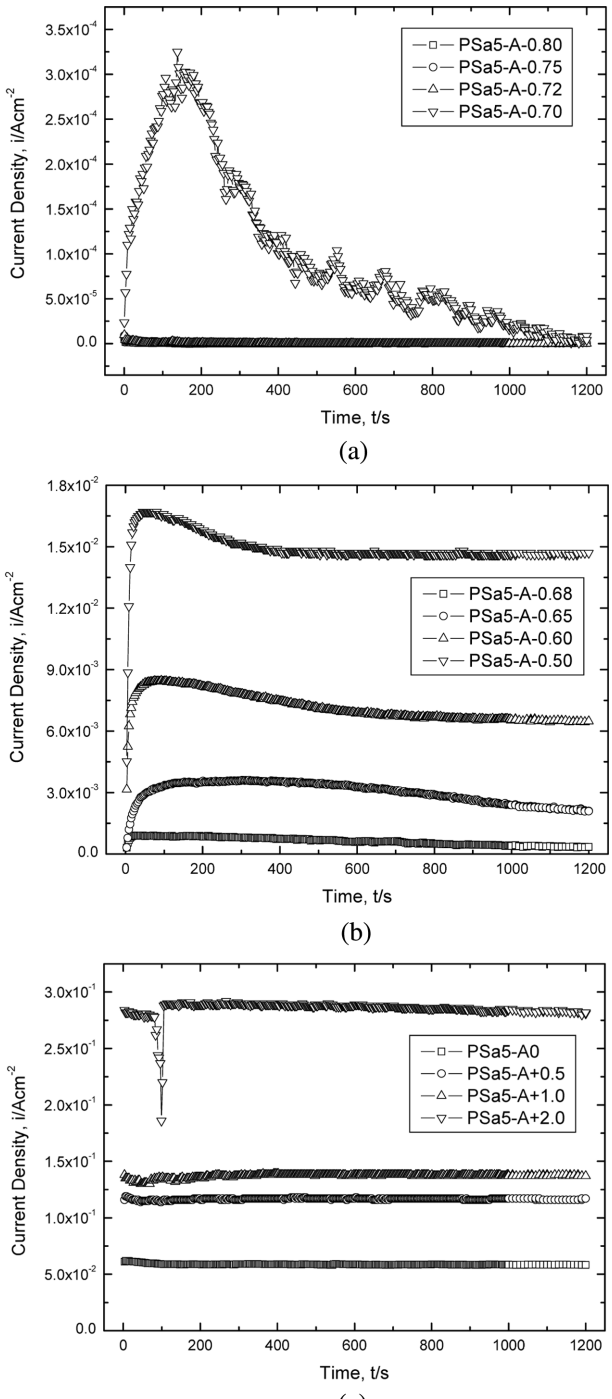

Fig. 4. Time-current density curves during potentiostatic experiment for 5456 specimen in natural sea water solution.

in a similar manner to that during anodic polarization, gradually increasing over the initial stages and attaining a maximum value at about 50 sec after which they remained more or less stable. The current densities after 1,200 sec were 6.48×10^{-3} A/cm^2 and 1.47×10^{-2} A/cm^2 at potentials of −0.60 and −0.50 V, respectively. As in the anodic polarization experiments, the potentiostatic current densities at 1,200 sec in the range of −0.68~−0.50 V attained their highest value at −0.50 V.

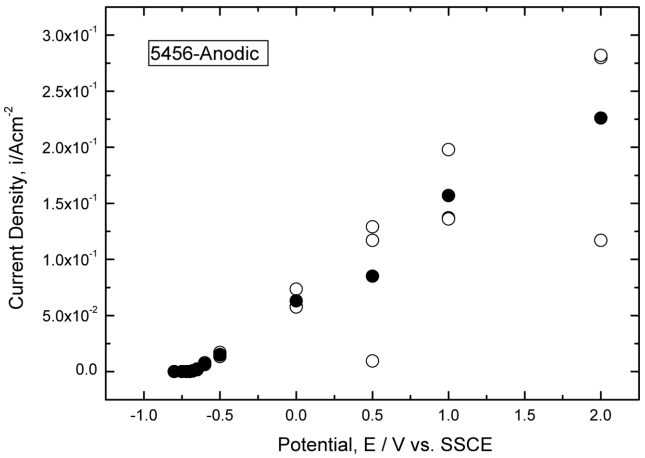

Fig. 5. Comparison of current density after potentiostatic experiment of 1200 s for 5456 specimen at various anodic potential in natural sea water solution.

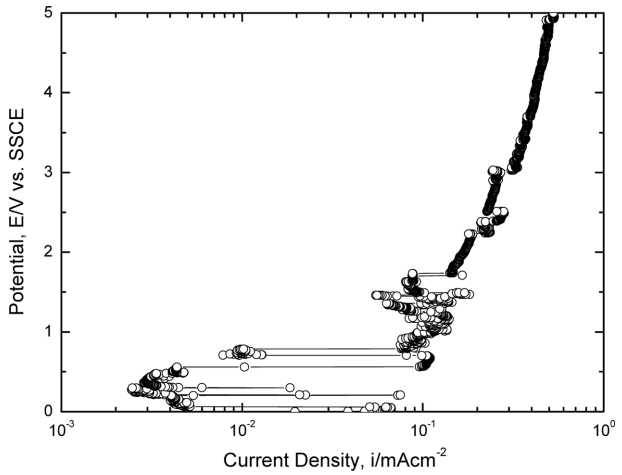

Fig. 6. Result of anodic polarization experiment to improve of corrosion by formation of anodic oxide film of 5456 alloy in natural sea water solution.

Potentiostatic experimental results in the range of 0-2.0 V are shown in Fig. 4(c). The reason that a low current density resulted at 0 V is due to formation of a passive film which was maintained up to 0.4 V. Above 0.4 V, the film is destroyed. As the potential increased from 0.5 to 1.0 V and then to 2.0 V, the current density after 1,200 sec increased. These potentiostatic results conform with the trends seen during anodic polarization.

Fig. 5 compares the current densities obtained in the potentiostatic experiments after 1,200 sec for all 5456 specimens analyzed at various anodic potentials in natural seawater. Each potentiostatic experimental run was executed several times, with the black circles representing the mean values found under the various conditions. The current densities in the range of −0.8~−0.68 V showed similar very low values in all experimental runs. At −0.65 V, the current density increased slightly, a trend that became more apparent at −0.5 V. Above −0.5 V, the current densities increased considerably with increasing potential. In particular, the current densities in the anodic polarization curves increased when the passive film was destroyed by the Cl^- in seawater. Thereafter, current densities decreased as passive films regrew. This phenomenon was repeated.

Fig. 6 shows the results of an anodic polarization experiment undertaken to ascertain how corrosion can be limited by formation of an anodic oxide film on 5456 alloy in seawater. A passivity trend was found to 0.6 V. When the passive film is destroyed by pitting, repassivity can occur repeatedly. Above 3 V, the passive film was destroyed entirely and a straight line increase occurred in current density.

Corrosion can similarly occur when hydrogen is generated at appropriate potentials in both acidic and alkaline solutions as shown in the E-pH diagram for aluminum [Pourbaix, 1974]. The pH of seawater is approximately 8.0 and the behavior of aluminum in seawater differs from that of aluminum in neutral solutions. Therefore, anticorrosive film was formed by the anodic oxide film in the neutral solution. It was concluded, however, that anticorrosive film due to anodization in seawater was not formed.

To date, the various trends involved in aluminum corrosion have been explored through anodic polarization. However, concentration polarization caused by the dissolved oxygen reduction reaction and

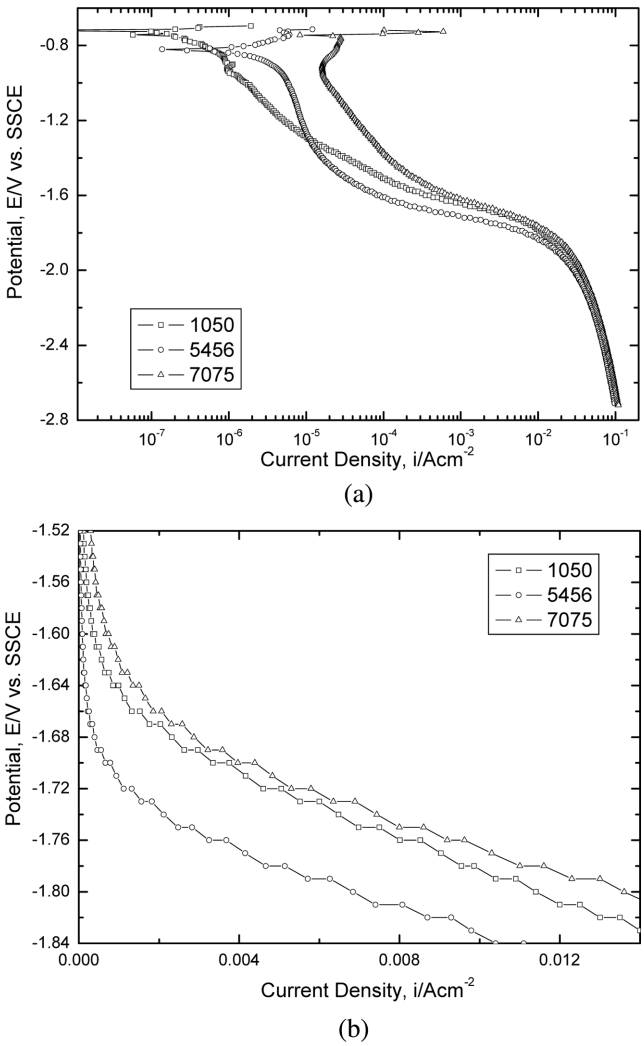

Fig. 7. Comparison of cathoodic polarization curves for 1050, 5456, 7075 specimens in natural sea water solution.

activation polarization caused by hydrogen generation are best understood by means of cathodic polarization analysis. To this end we have endeavored to ascertain the optimum protection potential range with respect to both hydrogen embrittlement and stress corrosion cracking.

Fig. 7 compares the results of cathodic polarization experiments for 1050, 5456, and 7075 specimens in seawater. The polarization trends for all three alloys show the effects of concentration polarization due to oxygen reduction ($O_2+2H_2O+4e^- \rightarrow 4OH^-$) and activation polarization due to hydrogen generation ($2H_2O+2e \rightarrow H_2+2OH^-$). The lowest value of current density for 1050 occurred above −1.3 V, but for 5456 was below −1.3 V. The highest current densities in all potential ranges of cathodic polarization occurred with 7075. Consequently, the usefulness of 7075 in marine environments is limited compared to 5456. The current density for passivity in anodic polarization is greater than that of dissolved oxygen reduction during cathodic polarization. This implies that, economically, cathodic protection is more beneficial than anodic protection. However, we also investigated if improvements in corrosion resistance could be obtained when Al was subjected to friction stir welding in order to relieve the residual stress due to heat [Jang et al., 2004]. Upon close examination, anodic protection of friction stir welding on the 1050 Al specimen was found to be more economical than that offered by cathodic protection. In investigations of hydrogen embrittlement in high-strength steel [Kim et al., 2002, 2003], the point at which the changeover takes place from concentration polarization due to oxygen reduction to activation polarization due to hydrogen generation is at approximately −1,000 mV (SCE). In the cathodic polarization Al, however, this changeover point is not clear and Fig. 7(b) has been recast to allow for a mutual comparison. This shows the changeover points for 1050, 5456, and 7075 Al alloys as being approximately −1.66, −1.7, and −1.64 V, respectively. That of 5456 alloy shows the lowest potential and that of 7075 the highest, meaning that 7075 alloy is most strongly affected by hydrogen embrittlement.

The electrochemical properties of 7075 alloy, when compared with 1050 and 5456 alloys, imply that the high strength of the metal goes hand in hand with considerable residual stress, and it can be concluded that the electrochemical properties of 5456 alloy make it superior to 7075, with the added bonus of 5456 undergoing repeated repassivity following destruction of its passive film when subjected to anodic polarization.

The current density for the potential at which hydrogen is generated during cathodic polarization increased abruptly. Investigations on hydrogen embrittlement of high-strength steel [Kim et al., 2002, 2003] have shown that the changeover from concentration polarization to activation polarization occurs at −1,000 mV (SCE). A potential of −900 mV (SCE) can also be included in the range at which concentration polarization occurs because the reaction involves the reduction of dissolved oxygen. However, hydrogen embrittlement can also occur at −900 mV when atomic hydrogen is present. To examine the possible effects of atomic hydrogen, potentiostatic experiments were conducted on the 5456 specimen.

Fig. 8 shows time-current density curves of potentiostatic experiments on 5456 in seawater. Fig. 8(a) shows the results at applied potentials of −1.5~−0.9 V, a potential range that includes that of dissolved oxygen reduction, i.e., that within the protection potential

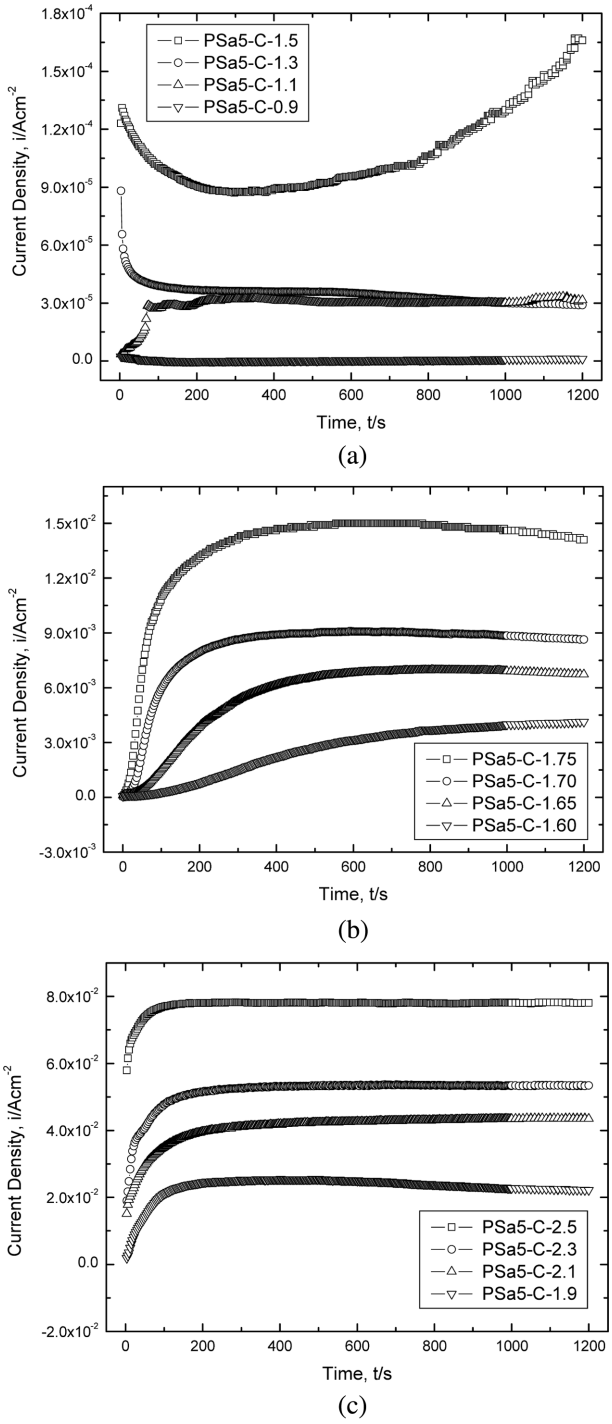

Fig. 8. Time-current density curves during potentiostatic experiment for 5456 specimen in natural sea water solution.

range. Current densities in the range of −1.3~−0.9 V showed stable values at around 100 sec with current densities at 1,200 sec of 2.9×10^{-5} A/cm^2, 3.15×10^{-5} A/cm^2, and 1.18×10^{-6} A/cm^2 at −1.3, −1.1, and −0.9 V, respectively. All current densities tended to be low. In spite of being within the protection potential range, the current density at −1.5 V during anodic polarization was slightly elevated at 1.66×10^{-4} A/cm^2. This increase possibly arose from the monatomic reaction of hydrogen ions ($H^+ + e \rightarrow H$) prior to activation polariza-

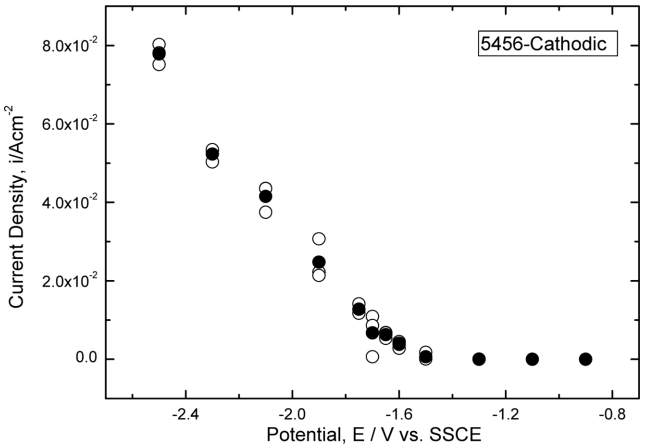

Fig. 9. Comparison of current density after potentiostatic experiment of 1200 s for 5456 specimen at various cathodic potential in natural sea water solution.

tion.

The results of potentiostatic experiments in the range of −1.75~−1.60 V, spanning the changeover from concentration polarization to activation polarization, are shown in Fig. 8(b). The current density increased with the potential shifts to a more negative value. This potential range corresponded to the generation of atomic hydrogen ($H^+ + e \rightarrow H$) or the production of molecular hydrogen from atomic hydrogen ($H^+ + e + H \rightarrow H_2$, $H + H \rightarrow H_2$). The upshot was acceleration of activation polarization and an increase in current density. We concluded that atomic hydrogen affected the potential at which the changeover occurred.

Fig. 8(c) shows the potentiostatic results in the range of −2.5~−1.9 V. The current density increased with an increase in negative potential and the increase in current density was linear, with activation polarization intensifying the generation of hydrogen due to cathodic polarization that could be seen by the unaided eye. The effect of atomic hydrogen was smaller than that of molecular hydrogen.

A comparison of the current densities measured for 5456 alloy in seawater at the conclusion of each potentiostatic experiment at 1,200 sec is shown in Fig. 9 at various cathodic potentials. The potential range of −0.9~−1.3 V during cathodic polarization showed a low current density applicable to protection. At −1.5 V, the effects of atomic hydrogen are seen in a slightly elevated current density. The potential range of −1.6~−1.75 V corresponded to the changeover from dissolved oxygen reduction to the activation reaction, and was affected by the presence of both atomic hydrogen and molecular hydrogen. We concluded, however, that effects on the current density from atomic hydrogen were small. Current densities in the range of −1.9~−2.5 V increased abruptly with any shift toward the active direction and it seems likely that their high current densities reflected the presence of molecular hydrogen. This was the same trend observed in cathodic polarization.

Fig. 10 compares the current densities in potentiostatic experiments conducted for 1,200 sec at various polarization potentials in seawater. In the potential range from −0.68 to −1.5 V, current densities were low and gave an estimate of the viable protection potential range. This is illustrated in greater detail in Fig. 10(b).

The current density increased suddenly when the applied potential shifted beyond the protection potential range in either the anodic or cathodic directions. In general, it was found that the high-strength 7075 alloy showed the highest current densities. This is the alloy most prone to stress corrosion cracking and hydrogen embrittlement. The main reason that residual stress in 7075 is high is the alloy's high strength, also seen in the great hardness of 7075 compared with 1050 and 5456. In comparison, 5456 alloy is less prone to stress corrosion cracking and hydrogen embrittlement in seawater due to its low current density.

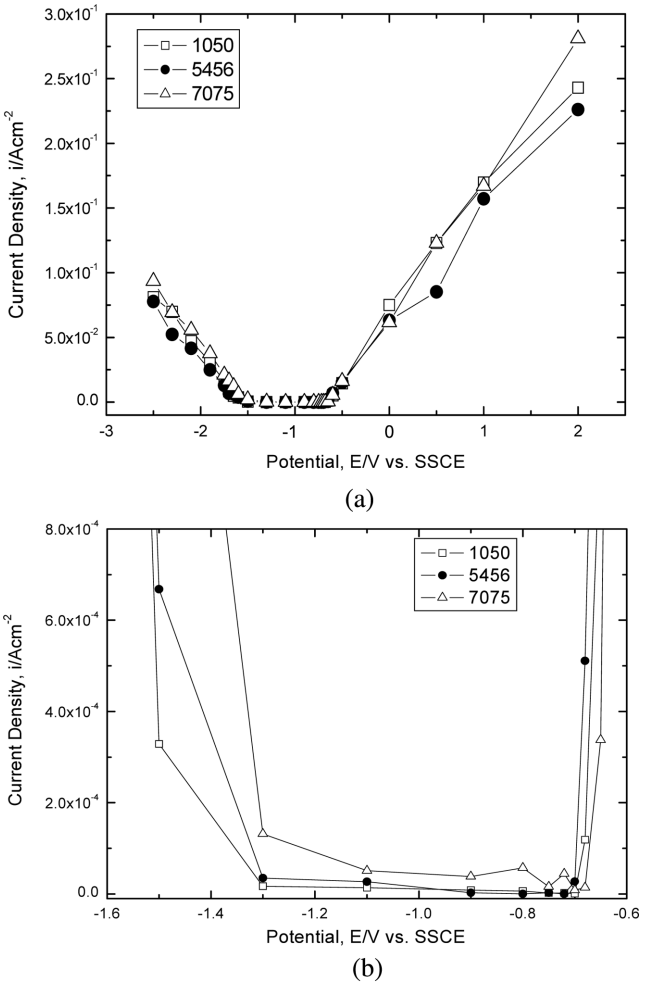

Fig. 10. Comparison of current density after potentiostatic experiment for 1200 s at various polarization potential in natural sea water solution.

Fig. 10(b) shows a magnified view of Fig. 10(a) within the potential range of −1.5~−0.68 V. In general, the current density of 7075 Al alloy was high compared to 1050 and 5456. The optimum protection potential in the potential range of −1.5~−0.68 V for 5456 alloy was obtained between −0.70 and −1.3 V, when current densities were very low. According to the criteria for cathodic protection given by England (CP 1021) [Jeon, 1985], the protection potential of Al is −0.85~−1.1 V (SSCE), with pitting not occurring at a cathodic polarized potential of about 0.15 V compared to the OCP. During potential measurement experiments conducted over 24 hours in this study, at potentials in the range of −0.69~−0.72 V, agreement was found with England's criteria for cathodic protection for

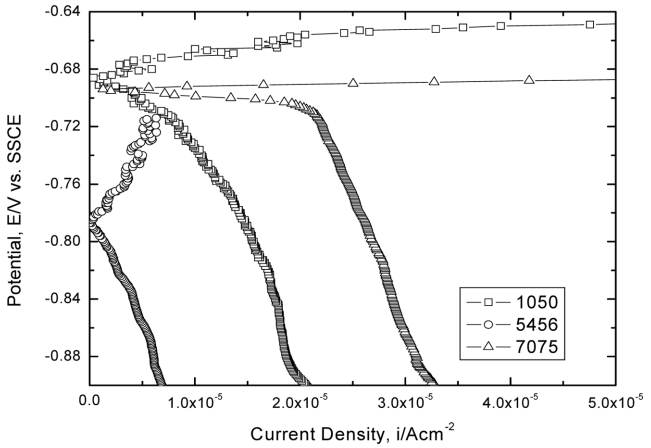

Fig. 11. Results of Tafel analysis for 1050, 5456 and 7075 in natural sea water solution.

Table 2. Results obtained from Tafel analysis of 1050, 5456, and 7075 Al alloys in seawater

	Corrosion potential (mV)	Corrosion current density (A/cm^2)
1050	−686	1.18×10^{-6}
5456	−787	4.0×10^{-7}
7075	−694	2.05×10^{-5}

alloy 1050, the current densities remaining very low at all potentials. This is considered to be the principal reason for the low residual stress of 1050 Al.

Fig. 11 shows the polarization curves resulting from Tafel analysis of alloys 1050, 5456, and 7075 in seawater. The corrosion potential of 5456 alloy was far lower than any other Al product, as were its corrosion current densities. The polarization behavior of 1050 was similar to that of 7075. The corrosion potential of 1050 was noble compared to that of 7075. Furthermore, the corrosion current density of 1050 Al was low compared to that of 7075. Consequently, the electrochemical properties of 1050 Al in seawater were better than those of 7075, with the trend of its corrosion potential being identical to the potential trend shown in Fig. 2. In brief, 5456 Al alloy is widely used in marine environments because its current density is the lowest at any given potential. While the 1050 alloy shows good anticorrosion characteristics, its practical uses are limited because its hardness is very low. Table 2 lists the results of the Tafel analysis in detail.

The current densities in all experiments undertaken to ascertain electrochemical properties returned very low values in the passivity range as well as in the potential range in which concentration polarization by dissolved oxygen reduction occurs. It is estimated, however, that stress corrosion cracking and hydrogen embrittlement will develop when high current densities result from contamination of seawater. Further investigations are planned to ascertain the optimum protection conditions in seawater to prevent stress corrosion cracking and hydrogen embrittlement arising from slow strain rates, as well as the optimum protection potentials required to maximize passivity and dissolved oxygen reduction at constant currents.

CONCLUSIONS

A study of the electrochemical properties of Al and Al alloys in seawater found that:

Current densities in 7075 Al alloy increase linearly with increasing potential during anodic polarization. In 1050 and 5456 alloys, passive films developed during anodic polarization are destroyed by Cl^- in the seawater, but repeatedly reform to make the Al alloy self-healing. On the whole, current densities in 5456 Al alloy are lower than that 1050. Cathodic polarization results in concentration polarization by dissolved oxygen reduction and activation polarization as a result of hydrogen generation. The changeover occurs at −1.66, −1.70, and −1.64 V (SSCE) in 1050, 5456, and 7075, respectively. Current densities increase suddenly in both anodic and cathodic directions beyond the potential range of −1.5~−0.68 V. Current density is highest in high-strength 7075 Al alloy while that in 5456 alloy is the lowest (−0.70~−1.3 V), making it the most corrosion-resistant in seawater environments. Consequently, optimum protection occurs in the potential range of −0.70~−1.3 V.

REFERENCES

Cho, J. H., *Korea research institute of medium and small shipbuilding*, **10**, 6 (2004).

Inoue, T. and Oki, T., "Characterization of passivation film on surface of aluminum alloy by heat-treatment," *Journal of Japan Institute of Heat Treatment*, **34**(2), 110 (1994).

Jang, S. K., Lee, D. C., Kim, S. J., Jeon, J. I. and Kim, S. H., "Investigation of macrostructures and properties for friction stir welded 1050 aluminum alloy sheet," *The proceeding of Korean Society of Marine Engineers*, 139 (2004).

Jeon, D. H., *Control of corrosion and protection*, 316, Il-Joong publishing Co. (1985).

Kanematsu, H., Okido, M. and Oki, T., "Electrochemical study on stress corrosion cracking of Al-Zn-Mg alloy," *Journal of Japan Institute of Light Metals*, **36**(3), 125 (1986).

Kanematsu, H., Okido, M. and Oki, T., "The effects of heat treatments on the SCC susceptibility of Al-Zn-Mg alloy," *Journal of Japan Institute of Light Metals*, **36**(5), 255 (1986).

Kang, B. Y. and Cho, J. H., "Consideration for structure and fabrication procedure of Al boat," *The Korean Journal of Welding Society*, **22**(3), 39 (2004).

Kim, S. J. and Moon, K. M., "Hydrogen embrittlement properties of heat affected zone of high strength steel in shielded metal arc welding," *Metals and Materials International*, **8**(4), 395 (2002).

Kim, S. J. and Moon, K. M., "The relationship between corrosion protection and hydrogen embrittlement properties of HAZ in flux cored arc welding," *Metals and Materials International*, **8**(4), 387 (2002).

Kim, S. J., Okido, M. and Moon, K. M., "An electrochemical study of cathodic protection of steel used for marine structures," *Korean J. Chem. Eng.*, **20**, 560 (2003).

Kim, S. J., Okido, M. and Moon, K. M., "The electrochemical study on mechanical and hydrogen embrittlement properties of HAZ part as a function of post-weld heat treatment in SMAW," *Surface and coatings Technology*, **169-170**, 163 (2003).

Pourbaix, M., "Atlas of electrochemical equilibria," *NACE*, 168 (1974).